THE JOURNAL OF PHYSICAL CHEMISTRY C

Article

pubs.acs.org/JPCC

High Coverage CO Activation Mechanisms on Fe(100) from Computations

Tao Wang,[†] Xinxin Tian,[‡] Yong-Wang Li,[‡] Jianguo Wang,[‡] Matthias Beller,[†] and Haijun Jiao*[,†,‡]

[†]Leibniz-Institut für Katalyse e.V. an der Universität Rostock, Albert-Einstein Strasse 29a, 18059 Rostock, Germany

[‡]State Key Laboratory of Coal Conversion, Institute of Coal Chemistry, Chinese Academy of Sciences, Taiyuan, Shanxi 030001, PR China

Supporting Information

ABSTRACT: CO activation on Fe(100) at different coverage was systematically computed on the basis of spin-polarized density functional theory. At the saturated coverage (11CO) on a $p(3 \times 4)$ surface size (24 exposed Fe atoms), top (1CO), bridge (3CO) and 4-fold hollow (7CO) adsorption configurations coexist. The stepwise adsorption energies and dissociation barriers at different coverage reveal equilibriums between desorption and dissociation of adsorbed CO molecules. It is found that only molecular adsorption is likely for n_{CO} = 8−11, and mixed molecular and dissociative adsorption becomes possible for n_{CO} = 5−7, while only dissociative adsorption is favorable for n_{CO} = 1−4. The computed CO adsorption configurations and stretching frequencies as well as desorption temperatures from ab initio thermodynamic analysis agree well with the available experimental data.

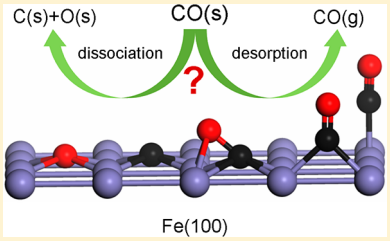

1. INTRODUCTION

In our modern daily life, CO is a very important basic chemical which has been widely applied in energy societies as well as value-added bulk and fine chemical productions. Representative examples are liquid fuels and chemicals from Fischer−Tropsch synthesis (FTS), methanol and synthetic natural gas as well as hydrogen.[1,2] Since all these chemical processes are conducted on the basis of heterogeneous catalysis; studying CO activation mechanisms on surfaces of solid catalysts can provide the essential and intrinsic information for understanding such key processes.

The interaction of CO on iron surfaces is of particular importance for understanding the initial steps in iron-based FTS, since CO dissociation is believed to be essential for CH_x formation.[3,4] Diverse experimental techniques were applied to study CO adsorption on iron single crystalline surfaces. On Fe(100), X-ray photoelectron spectroscopy (XPS) and temperature programmed desorption (TPD) studies[5−7] showed that there are three molecular adsorption states (α_1, α_2 and α_3) and CO dissociation occurs at about 440 K, while recombinative desorption of the dissociated C and O takes place at around 750−800K (β state). Further study by applying extensive surface science techniques, such as XPS, TPD, X-ray photoelectron diffraction (XPD),[8] near-edge X-ray absorption fine structure spectroscopy (NEXAFS),[9−11] and high resolution electron energy loss spectroscopy (HREELS)[12,13] revealed that the 4-fold hollow site with an unusually low CO stretching frequency of 1210 cm^{-1} is the most stable adsorption configuration, which corresponds to the α_3 state and represents the precursor state of CO dissociation. By using HREELS and temperature programmed surface reaction (TPSR) techniques, Lu et al.[14] studied CO adsorption and dissociation on the Fe(100) surface at 423 K, and found CO dissociation at coverage lower than 0.15 monolayer (ML), and CO desorption at coverage higher than 0.15 ML. The bonding mechanism of the predissociative hollow (α_3) phase and the nondissociative atop (α_1) phase of CO on the Fe(100) surface was studied by Gladh et al.[15] by using both X-ray emission spectroscopy (XES) and density functional theory (DFT) calculations, and a π donation/π^* back-donation scheme is proposed for CO in the 4-fold hollow site.

In addition to the extensive experimental studies, CO interaction on iron single crystalline surfaces has been also widely studied theoretically. Early theoretical studies mainly applied semiempirical[16,17] and Hatree-Fock[18] methods in 1980s. By using both periodic slab and finite cluster models to study CO adsorption on the Fe(001) surface, Nayak et al.[19] found that the 4-fold hollow site is the energetically most preferred adsorption site, followed by the atop and bridge sites. By applying DFT calculations, Sorescu et al.[20] studied the adsorption of CO, C, and O atoms, as well as CO dissociation on the Fe(100) surface, respectively, and found that CO on the 4-fold site (α_3 state in TPD) is most stable and has dissociation barrier in the range of 24.5−28.2 kcal/mol, while CO on the bridge site (α_2 state) is more stable than on the atop site (α_1 state) at low coverage, and the atop site becomes more stable than the bridge site at high coverage. Bromfield et al.[21] studied CO interaction on the Fe(100) surface and found that CO adsorption and dissociation are coverage dependent. On the Fe(100) surface, Elahifard et al.[22] proposed CO direct

Received: October 18, 2013
Revised: December 15, 2013
Published: December 19, 2013

dissociation at low coverage, and H-assisted CO dissociation at high coverage.

Despite these extensive DFT studies about CO adsorption on the Fe(100) surface, combined DFT and experimental studies of the adsorption, desorption, and dissociation mechanisms are still scare. In this work we have carried out comprehensive DFT computations on the adsorption, dissociation, and desorption at different CO coverage. Our ultimate goal is to understand the coverage dependence of adsorption, dissociation, and desorption processes upon the change of temperature. A direct comparison between our computed results and the available experimental data provides insights into the interaction mechanisms of CO on iron surfaces.

2. COMPUTATIONAL METHODS AND MODELS

2.1. Methods. Calculations were done by using the plane-wave based density functional theory (DFT) method implemented in the Vienna Ab Initio Simulation Package (VASP)[23,24] and periodic slab models. The electron ion interaction was described with the projector augmented wave (PAW) method.[25,26] The electron exchange and correlation energy was treated within the generalized gradient approximation in the Perdew–Burke–Ernzerhof formalism (GGA-PBE).[27] Spin-polarization calculation was included for iron systems to correctly account for its magnetic properties, and this was found essential for an accurate description of adsorption energy.[28] An energy cutoff of 400 eV and a second-order Methfessel–Paxton[29] electron smearing with σ = 0.2 eV were used to ensure accurate energies with errors less than 1 meV per atom. The vacuum layer between periodically repeated slabs was set as 10 Å to avoid interactions among slabs. To locate the CO dissociation transition states on iron surfaces, the nudged elastic band (NEB)[30] method was applied, and stretching frequencies were analyzed to characterize a transition state with only one imaginary frequency.

The adsorption energy (E_{ads}) of one CO molecule is defined as $E_{ads} = E_{CO/slab} - [E_{slab} + E_{CO}]$, where $E_{CO/slab}$ is the total energy of the slab with one CO adsorption, E_{slab} is the total energy of the bare slab and E_{CO} is the total energy of a free CO molecule in gas phase; and a more negative E_{ads} indicates a stronger adsorption.

To discuss molecular CO adsorption on Fe(100) surface at different coverage, it is necessary to find the most stable coadsorption configurations at individual coverage; i.e., one additional CO molecule was added to the previous most stable one for getting the next most stable one after considering all adsorption sites. In order to get the saturated coverage, we used the stepwise adsorption energy, $\Delta E_{ads} = E_{(CO)n+1/slab} - [E_{(CO)n/slab} + E_{CO}]$, where a positive ΔE_{ads} for $n + 1$ adsorbed CO molecules indicates the saturated adsorption with n CO molecules.

The CO dissociation barrier (E_a) is defined as $E_a = E_{TS} - E_{IS}$, the reaction energy (E_r) is defined as $E_r = E_{FS} - E_{IS}$, where E_{IS}, E_{FS}, and E_{TS} represent the total energy of the initial adsorbed CO molecule, final dissociated CO molecule (C+O atoms), and the CO dissociating transition states.

2.2. Models. Calculation of the α-Fe bulk crystal structure with a k-point mesh of 9 × 9 × 9 gives a lattice constant of 2.84 Å and a local spin magnetic moment of 2.214 μ_B, in good agreement with other DFT calculations[31,32] and experiment.[33] In order to choose a reasonable slab model for CO adsorption and dissociation at high coverage, we have tested the effects of slab thickness, surface size, and vacuum layer on CO adsorption energy extensively, and all these benchmark results are listed in the Supporting Information. On the basis of these tests, we applied the surface p(3 × 4) model for our study with four atomic layers, in which the top two layers were allowed to relax and the bottom two layers were fixed in their bulk positions. The structure and possible adsorption sites of Fe(100) surface are shown in Figure 1

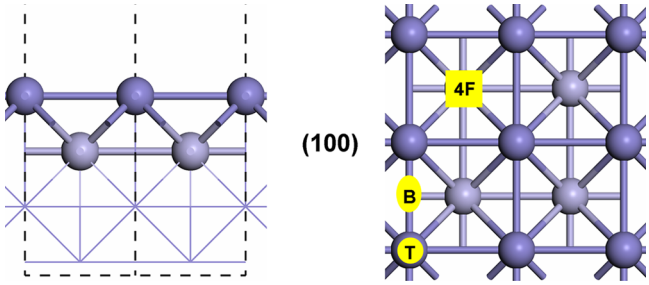

Figure 1. Schematic side and top views of Fe(100) and possible adsorption sites.

2.3. Thermodynamics. As a convenient tool to solve problems referring to real reaction conditions, *ab initio* atomistic thermodynamics method, proposed by Scheffler and Reuter,[34,35] has been widely and successfully applied in many other systems.[36−42] The detailed description of the method can be found in the Supporting Information.

3. RESULTS AND DISCUSSIONS

3.1. Molecular CO Adsorption at Saturated Coverage. There are three adsorption sites on the Fe(100) surface (Figure 1), i.e., top (**T**), bridge (**B**) and 4-fold hollow (**4F**) sites. The structures and energies (ΔE_{ads}) of the most stable adsorption sites for stepwise CO adsorption are given Figure 2. It is found that the most stable adsorption configurations for one CO molecule on this surface is located on the **4F** site with the C atom coordinating with four surface Fe atoms and the O atom interacting with two surface Fe atoms. The C–O bond length is elongated to 1.32 Å with respect to gaseous CO (1.14 Å), and the computed C–O stretching frequency is 1172 cm^{-1}. Experimentally, this adsorption configuration is assigned to the α_3 adsorption state from TDS. Our calculated adsorption energy (−2.14 eV) is similar with that (−2.17 eV) by Sorescu et al.,[43] since the same functional was used. However, results obtained with RPBE (−1.90 eV),[20] PW91 (−2.02 eV,[20] and −2.54 eV[21]) and cluster model (−1.62 eV)[19] show obvious differences due to their quite different methods and models.

From the most stable adsorption configuration of one CO, we further increased the number of adsorbed CO molecules on the surface. In order to find the most stable coadsorption configuration at high coverage, we checked different adsorption possibilities under consideration that 4-fold hollow adsorption is more stable than bridge adsorption, and bridge adsorption is more stable than top adsorption. At low coverage and at the same adsorption sites, the energy differences are rather small. At high coverage and due to their lateral repulsive interaction, however, the energy differences among these coadsorption states raise due to the change of the adsorption configuration from 4-fold site to the bridge site as well as to the top sites. Nevertheless, these changes do not affect our conclusion. All

dx.doi.org/10.1021/jp4103367 | J. Phys. Chem. C 2014, 118, 1095−1101

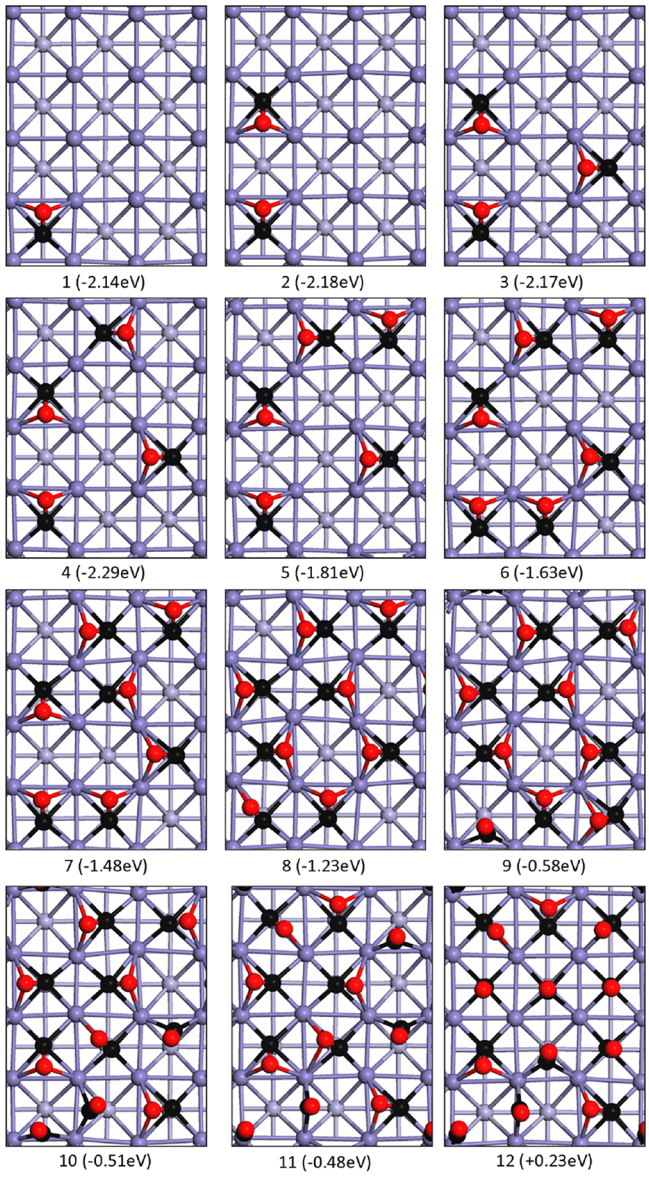

Figure 2. Structures and energies (ΔE_{ads}) of the most stable adsorption sites for stepwise CO adsorption (Blacks ball for C, red ball for O, and the other balls for Fe in different layers).

these preliminary data are summarized in the Supporting Information (Figure S1).

Figure 2 reveals that the first four adsorbed CO molecules (n_{CO} = 1−4) have the 4F adsorption configuration and very similar adsorption energies, indicating their negligible lateral repulsive interaction and their independence. With n_{CO} = 5−8, lateral repulsive interaction of the adsorbed CO molecules becomes significant and starts to affect the value of ΔE_{ads}, but all the adsorbed CO molecules still have the 4F adsorption configuration. With n_{CO} = 9, the bridge (B) adsorption configuration appears, and one B and eight 4F adsorption configurations coexist. With n_{CO} = 10, there are three B and seven 4F adsorption configurations. At the saturated coverage (n_{CO} = 11), there are one T, three B, and seven 4F adsorption configurations.

On the basis of the most stable adsorption configurations at a given coverage, it is interesting to compare the theoretically calculated and experimentally detected CO stretching frequencies. Early TPD studies[6] proved that there are three CO molecular desorption states (α_1, α_2 and α_3) at low temperature, and this supports our calculated result at the saturated coverage, where three adsorption configurations (one T, three B and seven 4F) coexist. Also HREELS[12,13] studies found three low temperature molecular adsorption states with quite different CO stretching frequencies, i.e., 1180−1245 cm^{-1} for the α_3 state and 1900−2070 cm^{-1} for the α_1 and α_2 states. Actually, our detailed analysis into CO stretching frequency at the saturated coverage also shows three ranges: 1179−1280 cm^{-1} for the 4F adsorption configuration, 1800−1850 cm^{-1} for the B adsorption configuration, and 2012 cm^{-1} for the **T** adsorption configuration. It clearly revealed that our calculated results are in good agreement with these available experimental data, indicating that our computed saturated coverage should be the same as found under experimental conditions.

3.2. Equilibrium between desorption and dissociation. In addition to the adsorption configurations at saturated coverage and their respective CO stretching frequencies, we are also interested in the desorption mechanisms of these adsorbed CO molecules at different coverage, in particular, the equilibrium between desorption and dissociation of the adsorbed CO molecules on the surface, for understanding the CO activation process.

To date, all theoretical studies are the subjects of CO adsorption and dissociation on iron surfaces at low coverage, and there are no investigations into the equilibrium between desorption and dissociation at different coverage. For the first time, we systematically computed CO dissociation at different coverage on the Fe(100) surface to find the equilibrium between desorption and dissociation. The calculated dissociation barriers of all adsorbed CO molecules on the basis of the most stable adsorption configurations in Figure 2 as the initial states at individual coverage are listed in Table 1, and the corresponding structures of initial states (IS), transition states (TS), and final states (FS) are given in the Supporting Information (Figure S2). For a direct and convenient comparison, we converted the calculated stepwise adsorption energies approximately to the reversed stepwise desorption energies. The potential energy surfaces at coverage of n_{CO} = 1−8 are shown in the Supporting Information (Figure S3).

Unlike the dissociation of one CO molecule, there are many possibilities for CO dissociation at high coverage. In order to find the energetically most favored one, we calculated the dissociation for all adsorbed CO molecules. For $n_{CO} \geq 2$, we calculated all CO dissociation barriers. After the dissociation of the first CO, the surface has $(n - 1)$ adsorbed CO molecules as well as one C atom and one O atom. The next step is to calculate the dissociation barriers of those $(n - 1)$ adsorbed CO molecules and to find the next most favorable one with $(n - 2)$ adsorbed CO molecules as well as two C atoms and two O atoms. The procedure was repeated till the CO desorption becomes more favorable than dissociation, and the final adsorption state could be identified.

To estimate the final adsorption state, it is necessary to consider the migration of surface C and O atoms, which is very important for understanding the complex oxidation and carburization of iron surface. Since there are free adsorption sites available at low coverage, and it is possible for C or O to migrate, and indeed, the barrier for one O migration is rather low (about 0.4 eV). At high coverage with adsorbed CO as well as C and O atoms, however, the surface has very limited free sites and considerable lateral repulsive interaction among the

dx.doi.org/10.1021/jp4103367 | J. Phys. Chem. C 2014, 118, 1095−1101

Table 1. CO Step Desorption Energies (ΔE_{des}, eV), and Dissociation Barriers (E_a, eV) As Well As Dissociation Energies (ΔE_{dis}, eV) at Different Coverage

nCO (ΔE_{des})	pathways	E_a	ΔE_{des}	ΔE_{dis}
1CO (2.14)	1CO → 1C + 1O	1.03	2.14	−1.20
2CO (2.18)	2CO → 1CO + 1C + 1O	1.04	2.18	−1.07
	1CO + 1C + 1O → 2C + 2O	1.12	2.06	−1.23
3CO (2.17)	3CO → 2CO+1C+1O	1.14	2.17	−1.18
	2CO+1C + 1O → 1CO + 2C + 2O	1.14	2.18	−0.88
	1CO + 2C + 2O → 3C + 3O	1.22	2.12	0.09
4CO (2.29)	4CO → 3CO + 1C+1O	1.17	2.29	−0.97
	3CO+1C+1O → 2CO + 2C + 2O	1.17	2.28	−0.83
	2CO+2C+2O → 1CO + 3C + 3O	1.25	2.28	−0.67
	1CO + 3C + 3O → 4C + 4O	1.31	2.40	0.25
5CO (1.81)	5CO → 4CO + 1C + 1O	1.13	1.81	−0.62
	4CO + 1C + 1O → 3CO + 2C + 2O	1.22	1.99	−0.03
	3CO + 2C + 2O → 2CO + 3C + 3O	1.22	1.48	−0.55
	2CO + 3C + 3O → 1CO + 4C + 4O	1.24	1.62	0.19
	1CO + 4C + 4O → 5C + 5O	2.48	1.30	0.17
6CO (1.63)	6CO → 5CO + 1C + 1O	1.20	1.63	−0.08
	5CO + 1C + 1O → 4CO + 2C + 2O	1.28	1.55	−0.40
	4CO + 2C + 2O → 3CO + 3C + 3O	1.25	1.56	0.06
	3CO + 3C + 3O → 2CO + 4C + 4O	1.46	1.12	0.25
	2CO + 4C + 4O → 1CO + 5C + 5O	2.44	0.49	−0.61
7CO (1.48)	7CO → 6CO + 1C + 1O	1.14	1.48	−0.28
	6CO + 1C + 1O → 5CO + 2C + 2O	1.31	1.52	−0.17
	5CO + 2C + 2O → 4CO + 3C + 3O	1.46	1.19	0.47
	4CO + 3C + 3O → 3CO + 4C + 4O	1.44	1.19	0.44
	3CO + 4C + 4O → 2CO + 5C + 5O	1.57	0.48	0,17
	2CO + 5C + 5O → 1CO + 6C + 6O	2.21	0.57	0.20
8CO (1.23)	8CO → 7CO + 1C + 1O	1.44	1.23	−0.02
	7CO + 1C + 1O → 6CO + 2C + 2O	1.44	1.14	0.07
	6CO + 2C + 2O → 5CO + 3C + 3O	1.71	0.91	0.32
	5CO + 3C + 3O → 4CO + 4C + 4O	2.53	1.05	0.41

adsorbed species, thus the migration of surface C or O should be very difficult.

For n_{CO} = 1, the computed CO dissociation barrier is much lower than own desorption energy (1.03 vs 2.14 eV), and CO dissociation is exothermic by 1.20 eV, indicating that CO dissociation is favorable both kinetically and thermodynamically. Our results agree well with the available results from literatures.[20,21,43]

For n_{CO} = 2, the dissociation barriers of these two CO molecules (1.04 and 1.12 eV) are lower than their corresponding desorption energies (2.18 and 2.06 eV), and the stepwise dissociation is exothermic by 1.07 and 1.23 eV, respectively. This shows that CO dissociation at this coverage is also favorable both kinetically and thermodynamically.

For n_{CO} = 3, the dissociation barriers of these three CO molecules (1.14, 1.14, and 1.22 eV) are lower than their corresponding desorption energies (2.17, 2.18, and 2.12 eV), and the dissociation of the first two CO molecules is exothermic by 1.18 and 0.88 eV, respectively, while that of the third CO molecule becomes slightly endothermic by 0.09 eV.

For n_{CO} = 4, the dissociation barriers of these four CO molecules (1.17, 1.17, 1.25, and 1.31 eV) are lower than their corresponding desorption energies (2.29, 2.28, 2.28, and 2.40 eV), and the dissociation of the first three CO molecules is exothermic by 0.97, 0.83, and 0.67 eV, respectively, while that of the fourth CO molecule is endothermic by 0.25 eV.

In contrast with the results for n_{CO} = 1−4, different results have been found for n_{CO} = 5−7. For n_{CO} = 5, the dissociation barriers of the first four CO molecules (1.13−1.24 eV) are lower than their corresponding desorption energies (1.48−1.99 eV). However, the dissociation barrier of the fifth CO molecule (2.48 eV) is much higher not only than own desorption energy (1.30) but also than the dissociation barriers of the first four CO molecules. This indicates that the fifth CO molecule prefers desorption from the surface instead of dissociation on the surface. Consequently, the final adsorption state has one adsorbed CO molecule as well as four C and four O atoms (CO + 4C + 4O) on the surface.

Very similar results are also found for n_{CO} = 6; i.e., the dissociation barriers of the first three CO molecules (1.20−1.28 eV) are much lower than their corresponding desorption energies. At this coverage, three adsorbed CO molecules desorb from the surface, and three adsorbed CO molecules dissociate on the surface. The final adsorption state has three adsorbed CO molecules as well as three C and three O atoms (3CO+3C +3O) on the surface.

For n_{CO} = 7, the dissociation barriers of the first two CO molecules are lower than their corresponding desorption energies while the further dissociation of other adsorbed CO become less favorable than desorption. The final adsorption state has five adsorbed CO molecules as well as two C and two O atoms (5CO + 2C + 2O) on the surface. The most favored potential energy surface of CO adsorption and dissociation at this coverage is given in Figure 3. It clearly reveals that a possible equilibrium between CO desorption from the surface and dissociation on the surface at the coverage of n_{CO} = 5−7.

For n_{CO} = 8, although the dissociation of the first three CO molecules (1.44−1.71 eV) are much lower than that of the fourth CO molecule (2.53 eV), they are higher than their corresponding desorption energies. Therefore, at this coverage, the first step should be CO desorption instead of dissociation. The final adsorption state has eight adsorbed CO molecules. It is to expect that at high coverage $n_{CO} \geq 8$, only desorption is possible because of the much low desorption energies. The final adsorption states have only adsorbed CO molecules.

These results reveal clearly that at coverage higher than $n_{CO} \geq 8$, the first step of the reaction is desorption of some adsorbed CO molecules from the surface. At coverage of n_{CO} = 7, both CO desorption from the surface and dissociation on the surface are possible, and they might form equilibrium. At coverage of n_{CO} = 5, 6, four of the adsorbed CO molecules can dissociate on the surface, and the rest of the adsorbed CO molecules desorb from the surface. At coverage of n_{CO} = 1−4, all adsorbed CO molecules can dissociate on the surface. A general trend shows that the adsorbed CO molecules prefer dissociation on the surface at low coverage, desorption from the surface at high coverage, and both CO desorption and dissociation can form equilibrium at coverage in between.

dx.doi.org/10.1021/jp4103367 | J. Phys. Chem. C 2014, 118, 1095−1101

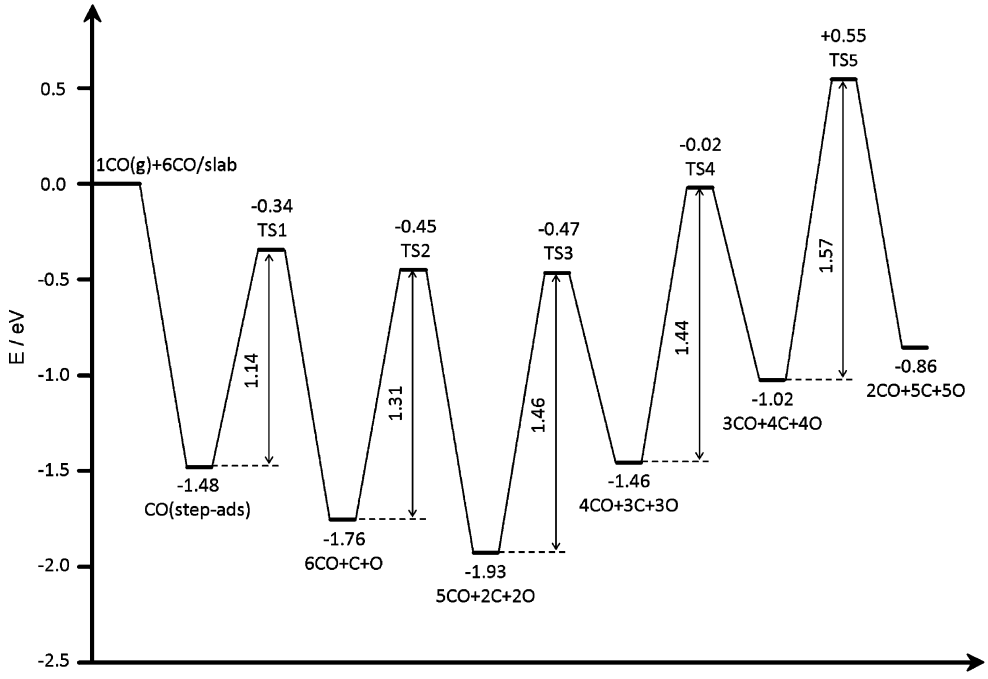

Figure 3. Potential energy surfaces of CO dissociation at the coverage of 7CO.

3.3. CO Desorption States and Temperatures on Fe(100). On the basis of our above results, we have computed the molecular desorption states (α_1-α_3) and the recombinative desorption state (β) under the consideration of CO dissociation at low coverage and high temperature from ab initio thermodynamics. Table 2 shows the good agreement between theory and experiment in CO desorption temperature at different coverage on Fe(100) surface under ultrahigh vacuum condition (10^{-10}Torr). For the first two molecular desorption states, α_1 state shows the loss of one T adsorbed CO molecule at 275−300K, and α_2 state indicates the loss of two B adsorbed CO molecules at 325−375 K. At 400−450 K with the coverage of eight 4F adsorbed CO molecules (8CO), desorption and dissociation take place simultaneously, and four CO molecules desorb, and the other four CO molecules dissociate. Finally the recombinative desorption (β state) of the dissociative adsorbed 4C and 4O atoms takes place at 700−750 K.

Table 2. CO Desorption Mechanisms at Different Coverage and Temperature

state	coverage	T^a	T^b
α_1	$11CO_{(s)} \rightarrow 10CO_{(s)} + 1CO_{(g)}$	275−300 K	220−250 K
α_2	$10CO_{(s)} \rightarrow 8CO_{(s)} + 2CO_{(g)}$	325−375 K	306−340 K
α_3	$8CO_{(s)} \rightarrow 4C_{(s)} + 4O_{(s)} + 4CO_{(g)}$	400−450 K	400−440 K
β	$4C_{(s)} + 4O_{(s)} \rightarrow 4CO_{(g)}$	700−750 K	750−820 K

[a]Theory. [b]Experiment.

On the basis of the identified most stable molecular and dissociative CO adsorption states at different coverage, we plotted the phase diagram to show the influence of temperatures and CO partial pressures (Figure 4). The phase diagram has four regions: from the only molecular adsorption to the mixed molecular and dissociative CO adsorption, as well as to the full dissociative adsorption and full desorption.

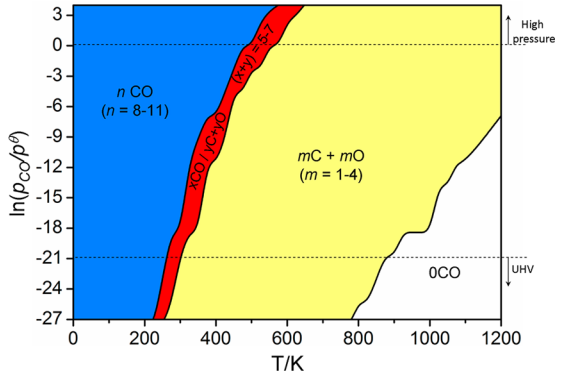

Figure 4. Equilibrium phase diagram of stable CO adsorption or dissociation states.

Apart from the agreement between theory and experiment in the three molecular adsorption states at low temperature,[6] the calculated CO dissociative adsorption also agrees with the experiments. For example, our results show full CO dissociation at the coverage with n_{CO} = 1−4. Considering the 24 exposed Fe atoms on the p(3 × 4) surface, the corresponding coverage for CO dissociation is 0.042, 0.083, 0.125, and 0.167 ML for n_{CO} = 1−4, respectively. On the Fe(100) surface at 423 K, Lu et al.[14] found CO dissociation at coverage lower than 0.15 ML, and CO desorption at coverage higher than 0.15 ML from HREELS and temperature programmed surface reaction (TPSR) studies. In addition, we also found the mixed molecular and dissociative CO adsorption at higher coverage from 0.208 to 0.292 ML.

Most interestingly, the phase diagram also provides the information about CO adsorption and dissociation at high temperature and high partial pressure on the Fe(100) surface. Indeed, such information is directly associated with the initial stage of the iron-based FTS catalysts, where the surfaces are proved to be precovered with CO.[44−46] On the basis of the precovered Fe(100) surface with CO as well as C and O atoms, it will be interesting to study the effects of hydrogen in CO

dx.doi.org/10.1021/jp4103367 | J. Phys. Chem. C 2014, 118, 1095−1101

activation, either direct dissociation or hydrogen-assisted dissociation under real experimental condition.

4. CONCLUSION

Spin-polarized density functional theory computations have been carried out to study the adsorption, dissociation, and desorption of CO on the Fe(100) surface at different coverage. Within the framework of a $p(3 \times 4)$ surface size (24 exposed surface Fe atoms), the most stable adsorption configuration changes from the 4-fold hollow site at low coverage (n_{CO} = 1−8) to the coexisted bridge and 4-fold hollow sites at the coverage of 9CO to 10CO molecules. At the saturated coverage (11CO), the most stable adsorption configuration has the coexistence of top (1CO), bridge (3CO), and 4-fold hollow (7CO) adsorption sites. The diverse molecular CO adsorption configurations at different coverage and the respective stretching frequencies are in good agreement with the available experimental data from high resolution electron energy loss spectroscopy studies.

On the basis of the computed stepwise CO adsorption energies and dissociation barriers, equilibriums between molecular and dissociative adsorption have been found. At high coverage (n_{CO} = 8−11), only molecular CO adsorption is found. For n_{CO} = 5−7, mixed molecular and dissociative CO adsorption becomes possible. At low coverage (n_{CO} = 1−4), only dissociative CO adsorption is favorable. Ab initio thermodynamic analysis reveals three desorption states from molecular adsorptions (α_1 at 275−300 K; α_2 at 325−375 K and α_3 at 400−450 K) and one recombinative desorption state from dissociative adsorptions (β at 700−750 K). The computed desorption temperatures also agree well with the available experimental data from temperature programmed surface reaction studies.

These detailed studies into the CO activation mechanisms show the insights into the initial process of iron-based Fischer−Tropsch synthesis, where CO adsorption and dissociation as well as surface carburization play the essential roles in structures, stability and activity of the catalysts. The computed CO desorption energies and dissociation barriers at different coverage and temperature provide the basis for microkinetic modeling, which is of practical importance.

■ ASSOCIATED CONTENT

Supporting Information

Detailed description of atomistic thermodynamics method, structures, and energies of those less stable adsorption configurations at a given coverage (Figure S1), structures of IS, TS, FS (Figure S2), as well as potential energy surfaces (Figure S3) of CO dissociation at different coverage are included. This material is available free of charge via the Internet at http://pubs.acs.org.

■ AUTHOR INFORMATION

Corresponding Author

*E-mail: haijun.jiao@catalysis.de.

Notes

The authors declare no competing financial interest.

■ ACKNOWLEDGMENTS

This work was supported by National Natural Science Foundation of China (No. 21273262), National Basic Research Program of China (No. 2011CB201406), Chinese Academy of Sciences and Synfuels CHINA. Co., Ltd. We also acknowledge general finical support from the BMBF and the state of Mecklenburg-Western Pommerania.

■ REFERENCES

(1) Anderson, R. B. *The Fischer-Troposch Synthesis*, Academic Press, Orlando, FL, 1984, p 3.
(2) Kelly, R. D.; Goodman, D. W.; In: King, D. A.; Woodruff, D. P., Eds. *The Chemical Physics of Solid Surfaces and Heterogeneous Catalysis*; Elsevier: Amsterdam, 1982; Vol. 4, p 427.
(3) Fischer, F.; Tropsch, H. Die Erdölsynthese bei Gewöhnlichen Druck aus den Vergasungsprodkten der Kohlen. *Brennstoff Chem.* **1926**, *7*, 97−116.
(4) Brady, R. C., III; Pettit, R. Reactions of Diazomethane on Transition-Metal Surfaces and Their Relationship to The Mechanism of the Fischer−Tropsch Reaction. *J. Am. Chem. Soc.* **1980**, *102*, 6181−6184.
(5) Benziger, J.; Madix, R. J. The Effects of Carbon, Oxygen, Sulfur and Potassium Adlayers on CO and H2 Adsorption on Fe(100). *Surf. Sci.* **1980**, *94*, 119−153.
(6) Moon, D. W.; Dwyer, D. J.; Bernasek, S. L. Adsorption of CO on the Clean and Sulfur Modified Fe(100) Surface. *Surf. Sci.* **1985**, *163*, 215−229.
(7) Cameron, S.; Dwyer, D. J. A Study of π-Bonded CO on Fe(100). *Langmuir* **1988**, *4*, 282−288.
(8) Saiki, R. S.; Herman, G. S.; Yamada, M.; Osterwalder, J.; Fadley, C. S. Structure of an Unusual Tilted State of CO on Fe(001) from X-ray Photoelectron Diffraction. *Phys. Rev. Lett.* **1989**, *63*, 283−286.
(9) Moon, D. W.; Cameron, S.; Zaera, F.; Eberhardt, W.; Carr, R.; Bernasek, S. L.; Gland, J. L; Dwyer, D. J. A Tilted Precursor for CO Dissociation on the Fe(100) Surface. *Surf. Sci. Lett.* **1987**, *180*, L123−L128.
(10) Moon, D. W.; Bernasek, S. L.; Lu, J. P.; Gland, J. L; Dwyer, D. J. Activation of Carbon Monoxide on Clean and Sulfur Modified Fe(100). *Surf. Sci.* **1987**, *184*, 90−108.
(11) Dwyer, D. J.; Rausenberger, B.; Cameron, S. D.; Lu, J. P.; Bernasek, S. L.; Fischer, D. A.; Parker, D. H.; Gland, J. L. Fluorescence Yield Near Edge Spectroscopy of π-Bonded on Fe (100). *Surf. Sci.* **1989**, *224*, 375−385.
(12) Moon, D. W.; Bernasek, S. L.; Dwyer, D. J.; Gland, J. L. Observation of an Unusually Low CO Stretching Frequency on Fe(100). *J. Am. Chem. Soc.* **1985**, *107*, 4363−4364.
(13) Benndorf, C.; Krüger, B.; Thieme, F. Unusually Low Stretching Frequency for CO Adsorption on Fe(100). *Surf. Sci. Lett.* **1985**, *163*, L675−L680.
(14) Lu, J. P.; Albert, M. R.; Bernasek, S. L. Adsorption and Dissociation of CO on Fe(100) at Low Coverage. *Surf. Sci.* **1989**, *217*, 55−64.
(15) Gladh, J.; Öberg, H.; Li, J. B.; Ljungberg, M. P.; Matsuda, A.; Ogasawara, H.; Nilsson, A.; Pettersson, L. G. M.; Öström, H. X-ray Emission Spectroscopy and Density Functional Study of CO/Fe(100). *J. Chem. Phys.* **2012**, *136*, 034702−9.
(16) Mehandru, S. P.; Anderson, A. B. Binding and Orientations of CO on Fe(110), (100) and (111): A Surface Structure Effect From Molecular Orbital Theory. *Surf. Sci.* **1988**, *201*, 345−360.
(17) Blyholder, G.; Lawless, M. A Theoretical Study of the Site of CO dissociation on Fe(100). *Surf. Sci.* **1993**, *290*, 155−162.
(18) Meehan, T. E.; Head, J. D. A Theoretical Comparison of CO Bonding on the Fe(100) Surface. *Surf. Sci.* **1991**, *243*, L55−L62.
(19) Nayak, S. K.; Nooijen, M.; Bernasek, S. L. Electronic Structure Study of CO Adsorption on the Fe(001) Surface. *J. Phys. Chem. B* **2001**, *105*, 164−172.
(20) Sorescu, D. C.; Thompson, D. L.; Hurley, M. M.; Chabalowski, C. F. First-Principles Calculations of the Adsorption, Diffusion, and Dissociation of a CO Molecule on the Fe(100) Surface. *Phys. Rev. B* **2002**, *66*, 035416.
(21) Bromfield, T. C.; Ferre, D. C.; Niemantsverdriet, J. W. A DFT Study of the Adsorption and Dissociation of CO on Fe(100):

Influence of Surface Coverage on the Nature of Accessible Adsorption States. *Chem. Phys. Chem.* **2005**, *6*, 254−260.
(22) Elahifard, M. R.; Jigato, M. P.; Niemantsverdriet, J. W. Direct versus Hydrogen-Assisted CO Dissociation on the Fe(100) Surface: A DFT Study. *Chem. Phys. Chem.* **2012**, *13*, 89−91.
(23) Kresse, G.; Furthmüller, J. Efficiency of Ab-initio Total Energy Calculations for Metals and Semiconductors Using a Plane-Wave Basis Set. *Comput. Mater. Sci.* **1996**, *6*, 15−50.
(24) Kresse, G.; Furthmüller, J. Efficient Iterative Schemes for Ab initio Total-Energy Calculations Using a Plane-Wave Basis Set. *Phys. Rev. B* **1996**, *54*, 11169−11186.
(25) Blochl, P. E. Projector Augmented-Wave Method. *Phys. Rev. B* **1994**, *50*, 17953−17979.
(26) Kresse, G. From Ultrasoft Pseudopotentials to the Projector Augmented-Wave Method. *Phys. Rev. B* **1999**, *59*, 1758−1775.
(27) Perdew, J. P.; Burke, K.; Ernzerhof, M. Generalized Gradient Approximation Made Simple. *Phys. Rev. Lett.* **1996**, *77*, 3865−3868.
(28) Kresse, G.; Hafner, J. First-Principles Study of the Adsorption of Atomic H on Ni (111), (100) and (110). *Surf. Sci.* **2000**, *459*, 287−302.
(29) Methfessel, M.; Paxton, A. T. High-Precision Sampling for Brillouin-zone Integration in Metals. *Phys. Rev. B* **1989**, *40*, 3616−3621.
(30) Henkelman, G.; Jónsson, H. Improved Tangent Estimate in the Nudged Elastic Band Method for Finding Minimum Energy Paths and Saddle Points. *J. Chem. Phys.* **2000**, *113*, 9978−9985.
(31) Jiang, E.; Carter, E. A. Carbon Dissolution and Diffusion in Ferrite and Austenite from First Principles. *Phys. Rev. B* **2003**, *67*, 214103−214113.
(32) Sorescu, D. C. First-Principles Calculations of the Adsorption and Hydrogenation Reactions of CHx (x = 0,4) Species on a Fe(100) Surface. *Phys. Rev. B* **2006**, *73*, 155420−155436.
(33) Kittel, C. *Introduction to Solid State Physics*; Wiley: New York, 1996.
(34) Reuter, K.; Scheffler, M. Composition, Structure, and Stability of RuO2(110) as a Function of Oxygen Pressure. *Phys. Rev. B* **2001**, *65*, 035406.
(35) Reuter, K.; Scheffler, M. Composition and Structure of the RuO2(110) Surface in an O2 and CO Environment: Implications for the Catalytic Formation of CO2. *Phys. Rev. B* **2003**, *68*, 045407.
(36) Li, W. X.; Stampfl, C.; Scheffler, M. Insights into the Function of Silver as an Oxidation Catalyst by Ab Initio Atomistic Thermodynamics. *Phys. Rev. B* **2003**, *68*, 165412.
(37) Rogal, J.; Reuter, K.; Scheffler, M. Thermodynamic Stability of PdO Surfaces. *Phys. Rev. B* **2004**, *69*, 075421.
(38) Grillo, M. E.; Ranke, W.; Finnis, M. W. Surface Structure and Water adsorption on Fe3O4(111): Spin-Density Functional Theory and On-Site Coulomb Interactions. *Phys. Rev. B* **2008**, *77*, 075407.
(39) Aray, Y.; Vidal, A. B.; Rodriguez, J.; Grillo, M. E.; Vega, D.; Coll, D. S. First Principles Study of Low Miller Index RuS_2 Surfaces in Hydrotreating Conditions. *J. Phys. Chem. C* **2009**, *113*, 19545−19557.
(40) Zasada, F.; Piskorz, W.; Cristol, S.; Paul, J. F.; Kotarba, A.; Sojka, Z. Periodic Density Functional Theory and Atomistic Thermodynamic Studies of Cobalt Spinel Nanocrystals in Wet Environment: Molecular Interpretation of Water Adsorption Equilibria. *J. Phys. Chem. C* **2010**, *114*, 22245−22253.
(41) Wang, T.; Liu, X. W.; Wang, S. G.; Huo, C. F.; Li, Y. W.; Wang, J. G.; Jiao, H. Stability of β-Mo2C Facets from Ab Initio Atomistic Thermodynamics. *J. Phys. Chem. C* **2011**, *115*, 22360−22368.
(42) Wang, T.; Wang, S. G.; Li, Y. W.; Wang, J. G.; Jiao, H. J. Adsorption Equilibria of CO Coverage on β-Mo2C Surfaces. *J. Phys. Chem. C* **2012**, *116*, 6340−6348.
(43) Sorescu, D. C. Plane-Wave DFT Investigations of the Adsorption, Diffusion, and Activation of CO on Kinked Fe(710) and Fe(310) Surfaces. *J. Phys. Chem. C* **2008**, *112*, 10472−10489.
(44) Mims, C. A.; McCandlish, L. E. Evidence for Rapid Chain Growth in the Fischer−Tropsch Synthesis over Iron and Cobalt Catalysts. *J. Phys. Chem.* **1987**, *91*, 929−937.
(45) Ojedaa, M.; Nabarb, R.; Nilekarb, A. U.; Ishikawaa, A.; Mavrikakisb, M.; Iglesia, E. CO Activation Pathways and the Mechanism of Fischer−Tropsch Synthesis. *J. Catal.* **2010**, *272*, 287−297.
(46) Loveless, B. T.; Buda, C.; Neurock, M.; Iglesia, E. CO Chemisorption and Dissociation at High Coverages during CO Hydrogenation on Ru Catalysts. *J. Am. Chem. Soc.* **2013**, *135*, 6107−6121.